Carbohydrate Polymers 95 (2013) 123–133

Contents lists available at SciVerse ScienceDirect

Carbohydrate Polymers

journal homepage: www.elsevier.com/locate/carbpol

Non-covalent crosslinkers for electrospun chitosan fibers

Marjorie A. Kiechel, Caroline L. Schauer*

Materials Science and Engineering Department, Drexel University, Philadelphia, PA 19104, USA

ARTICLE INFO

Article history:
Received 20 December 2012
Received in revised form 15 February 2013
Accepted 16 February 2013
Available online 26 February 2013

Keywords:
Chitosan
Electrospinning
Crosslinking
Tannic
Glycerol phosphate

ABSTRACT

Electrospun chitosan fibers have numerous potential in biomedical, food, and pharmaceutical applications. However, the mats formed are often not chemically stable in a wide range of pHs unless crosslinked. Here, we report on the use of glycerol phosphate (GP), tripolyphosphate (TPP) and tannic acid (TA) as a new set of non-covalent crosslinkers for electrospun chitosan fibers. Crosslinking with or without heat or base activation were performed either prior to (one-step or activated one-step) or after (two-step or activated two-step) electrospinning with either GP or TA. TPP crosslinking was performed in two-step and activated two-step. FESEM, FTIR and UV–vis transmittance at 600 nm were used to determine fiber surface morphology, chemical interactions and solubility in 1 M AA (pH 3), water (~pH 6) and 1 M NaOH (pH 13), respectively. Crosslinking of chitosan with GP and TA yields fibers with a mean diameter range of 145–334 nm and 143–5554 nm, respectively. TPP crosslinking produced branched fibers with mean diameters of 117–462 nm range. Two-step chitosan-TA did not dissolve in 1 M AA even after 72 h while all chitosan-TPP, activated two-step chitosan-TA and two-step heat activated chitosan-GP fibers survived in water after 72 h.

1. Introduction

Chitosan, the linear and partly acetylated (1-4)-2-amino-2-deoxy-β-D-glucan, is obtained from marine chitin (Muzzarelli, Boudrant et al., 2012). Chitosan possesses unique chemical properties owing to its cationic charge in solution and ability to form covalent or ionic bonds with other chemical species. These properties, along with the ease of chemically modifying and processing, remarkably increased the application-based research in pharmaceutical and biomedical engineering, water treatment and membrane systems (Kumar, Muzzarelli, Muzzarelli, Sashiwa, & Domb, 2004; Muzzarelli, Greco, Busilacchi, Sollazzo, & Gigante, 2012; Schiffman & Schauer, 2008).

Fine fibrous mats can be created from chitosan solutions through electrospinning. Electrospinning is a simple, low-cost and scalable method of producing polymer fibers with diameters reaching down to the nanometer scale, creating a mat with high surface area-to-volume ratio. The setup typically consists of three basic parts: (1) a needle-capped syringe containing the solution that is placed on an advancement pump; (2) a conductive collector; and (3) a high voltage power source that connects the needle and the collector. Fiber formation is influenced by solution, electrospinning and environmental parameters (Reneker, Yarin, Zussman, & Xu, 2007). When the applied voltage overcomes the polymer solution's opposing surface charge, the polymer jets out of the solution, elongates and whips due to charge instabilities and ultimately gets collected on the plate (Reneker et al., 2007; Schiffman & Schauer, 2008). Recently, we spun chitosan in trifluoroacetic acid (TFA), however the mat dissolves in neutral (pH 7) to acidic (~pH 3) conditions and thus requires crosslinking to improve its chemical stability for future applications (Schiffman & Schauer, 2007a, 2007b).

Chemically, the chitosan structure consists of D-glucosamine (deacetylated unit) and *N*-acetyl-D-glucosamine units. Under appropriate conditions, chitosan can form bonds with nearby chemical species due to either its protonated amine groups present on D-glucosamine or the primary and secondary hydroxyl groups (OH). One reaction can be the chemical crosslinking of chitosan, which is commonly performed on chitosan-based hydrogels, microspheres and films for use in various biomedical applications (Berger et al., 2004). Crosslinking modifies a few chitosan properties including chemical and mechanical stability (Austero, Donius, Wegst, & Schauer, 2012; Donius, Kiechel, Schauer, & Wegst, 2013; Schiffman & Schauer, 2007a, 2007b). There are a number of known ionic or covalently-binding chitosan crosslinkers but to date, only the covalent crosslinkers have been used to crosslink as-spun electrospun chitosan fibers in both one- and two-step method (Austero et al., 2012; Muzzarelli, 2009; Schiffman & Schauer, 2007a, 2007b).

In this study, we employed both one-step (OS) and two-step (TS) methods to expand the library of and demonstrate the chemical crosslinking techniques available for electrospun chitosan fibers. The OS method involves the addition of the crosslinker to the

* Corresponding author at: 3141Chestnut St. (LeBow 439A), Philadelphia, PA 19104, USA. Tel.: +1 215 895 6797; fax: +1 215 895 6760.
E-mail addresses: cschauer@coe.drexel.edu, cschauer@drexel.edu (C.L. Schauer).

0144-8617/$ – see front matter © 2013 Elsevier Ltd. All rights reserved.
http://dx.doi.org/10.1016/j.carbpol.2013.02.034

polymer solution before electrospinning, while TS is performed by immersing an as-spun polymer mat in a crosslinker solution. Schiffman and Schauer (2007a, 2007b) were the first to report on the difference between the OS and TS crosslinking of electrospun chitosan-GA on its fiber morphology, diameter and other mat properties.

OS method is advantageous as it allows better mixing of the polymer with the crosslinker before fiber formation and depending on the crosslinker reaction, may reduce the crosslinked fiber-processing step. A disadvantage however is that some crosslinkers like GA may readily crosslink chitosan at room temperature and in acidic conditions (i.e. the spinning solvent pH). This results in the solution forming a gel before fibers are formed, which adds an additional step to constantly replenish the solution with a newly mixed batch in order to get high fiber yields. The OS method also possesses a challenge if the addition of the crosslinker dramatically modifies the electrospinning solution properties, requiring adjustment in the electrospinning parameters. In contrast, TS crosslinking is advantageous as it allows ease in making the fibers before the crosslinking steps. Electrospinning parameters do not have to be adjusted however there is a need for this additional step after fiber formation.

Additionally, we introduce here heat or base activation for either OS or TS technique. A few crosslinkers, like HDACS (Austero et al., 2012), require either activation to fully crosslink. Similarly, some of the non-covalent crosslinkers used here require heat (60 °C) or base to fully crosslink.

In this paper, the aim is to investigate the use of glycerol phosphate (GP), tripolyphosphate (TPP) and tannic acid (TA) as a new set of stimulus-responsive crosslinkers for electrospun chitosan fibers. Previously spun chitosan crosslinked in either OS or TS approach yielded fibers with various fiber morphologies (Schiffman & Schauer, 2007a, 2007b). In this study, OS, activated OS, TS and activated TS methods of crosslinking of fibers and its influence in fiber morphology are also investigated.

Unlike our previously reported crosslinkers that form covalent bonds with chitosan (Austero et al., 2012), the crosslinkers GP, TPP and TA used here form ionic or hydrophobic interactions. Both GP, commercially sold as a sodium salt ($Na_2C_3H_7O_6P$), and the colorless inorganic sodium salt of TPP ($Na_5P_3O_4$) are phosphate-containing compounds that form networks by the electrostatic interactions of the negatively charged phosphate groups with the positively charged groups of the chitosan chains.

GP ($pK_{a\,(25\,^\circ C)}$ 6.26) (Fukada & Takahashi, 1998) is a thermosensitive crosslinker of chitosan hydrogels (Chenite, Buschmann, Wang, Chaput, & Kandani, 2001; Ruel-Gariepy, Chenite, Chaput, Guirguis, & Leroux, 2000) and films (Faikrua, Jeenapongsa, Sila-asna, & Viyoch, 2009).

Like GP, TPP is a common chitosan hydrogel crosslinker (Du, Niu, Xu, Xu, & Fan, 2009; Lopez-Leon, Carvalho, Seijo, Ortega-Vinuesa, & Bastos-Gonzalez, 2005; Shu & Zhu, 2001) owing to its highly charged phosphate groups ($P_3O_4{}^{5-}$). Other than electrostatic interactions, hydrophobic interactions and interchain hydrogen bonds (Brack, Tirmizi, & Risen, 1997; Ruel-Gariepy et al., 2000; Shu, Zhu, & Song, 2001) have also been reported to influence the crosslinked chitosan networks.

TA (pK_a 2.2–3.2) (Shutava, Prouty, Kommireddy, & Lvov, 2005) is a type of tannin, a naturally occurring plant polyphenol. It is a large glucose-containing molecule ($1.85 \times 1.65 \times 1.01\ nm^3$) (Madhan, Dhathathreyan, Subramanian, & Ramasami, 2003) that is esterified with phenols (gallic acid). Often reported as $C_{76}H_{52}O_{46}$ that corresponds to decagalloyl glucose, commercial TA is actually a mixture of polygalloyl glucose and polygalloyl quinic acid esters that has varying number of galloyl units, depending on its source. Tannins are known in nature to bind and precipitate polysaccharides (Charlton et al., 2002; Osawa & Walsh, 1993; Van Buren & Robinson, 1969). To date, the use of TA with chitosan has only been reported for films, microcapsules (Devi & Maji, 2009; Shutava et al., 2005; Shutava & Lvov, 2006) and adsorbent beads (An & Dultz, 2007; Chang & Juang, 2004). Although not yet fully understood, the possible binding mechanisms of TA to amine-containing polymers were considered to be due to the formation of hydrophobic or hydrogen bonds (Barry, Finkelstein, & Ross, 1984) or complexes (Van Buren & Robinson, 1969) that are influenced by temperature or pH (Charlton et al., 2002; Shutava et al., 2005).

2. Experimental

2.1. Reagents

Medium molecular weight chitosan (77% DD, MW = 190–310 kDa), trifluoroacetic acid (TFA, 99% ReagentPlus), glycerol-2-phosphate sodium dihydrate (GP), sodium tripolyphosphate (TPP) and tannic acid (TA) were used as received from Sigma Aldrich, MO, USA. Sodium hydroxide (NaOH), ethanol (200 Proof) and acetic acid (AA) from Sigma–Aldrich, MO, USA were also used for neutralization or solubility testing. All aqueous solutions were prepared with doubly distilled water.

2.2. Preparation of chitosan solutions

Solutions were prepared by mixing 3.7 wt.% chitosan in 99% TFA. The solutions were mixed for about 24 h at room temperature on an Arma Rotator A-1 (Bethesda, MD, USA). The electrospinning and crosslinking procedures were a modification of our previous work (Austero et al., 2012; Schiffman & Schauer, 2007b). All mats that were spun from chitosan solutions without additional crosslinkers were called as-spun mats.

2.3. Crosslinking methods

GP and TA were allowed to react with chitosan in four processing methods: (1) OS; (2) activated OS; (3) TS; and (4) activated TS while TPP utilized only TS and activated TS methods. For all methods of crosslinking, the polymer:crosslinker ratio was 3:1 (wt%) for GP (Faikrua et al., 2009), 4:1 (wt.%) for TPP (Shu & Zhu, 2000) and 1:1.4 (wt.%) for TA (Devi & Maji, 2009), except as indicated.

2.3.1. One-step (OS)

For this method, the crosslinker was added to the chitosan solution about 2 min prior to electrospinning.

2.3.2. Activated one-step

This was a modified version of the OS approach. Here, after spinning, the OS mats were either heat- or base-activated. Heat or base activation were carried out by exposing the mats to 60 °C in a convection oven for 24 h or in a gas vapor chamber (110 mm × 80 mm × 50 mm; VWR Scientific Products, Bridgeport, NJ) with 10 mL 1 M NaOH for 24 h at ambient conditions, respectively.

2.3.3. Two-step (TS)

The TS method was performed by the fabrication of as-spun mats followed by the immersion of the mats into the crosslinker solution. The as-spun mats were initially neutralized with freshly prepared 5 wt.% NaOH in ethanol for 1 h, washed with water until the wash solution is pH 7. Then, the mats were immersed into the aqueous crosslinker solution for 5 h at ambient conditions. Afterwards, the mats were rinsed with water until the wash solution was pH 7.

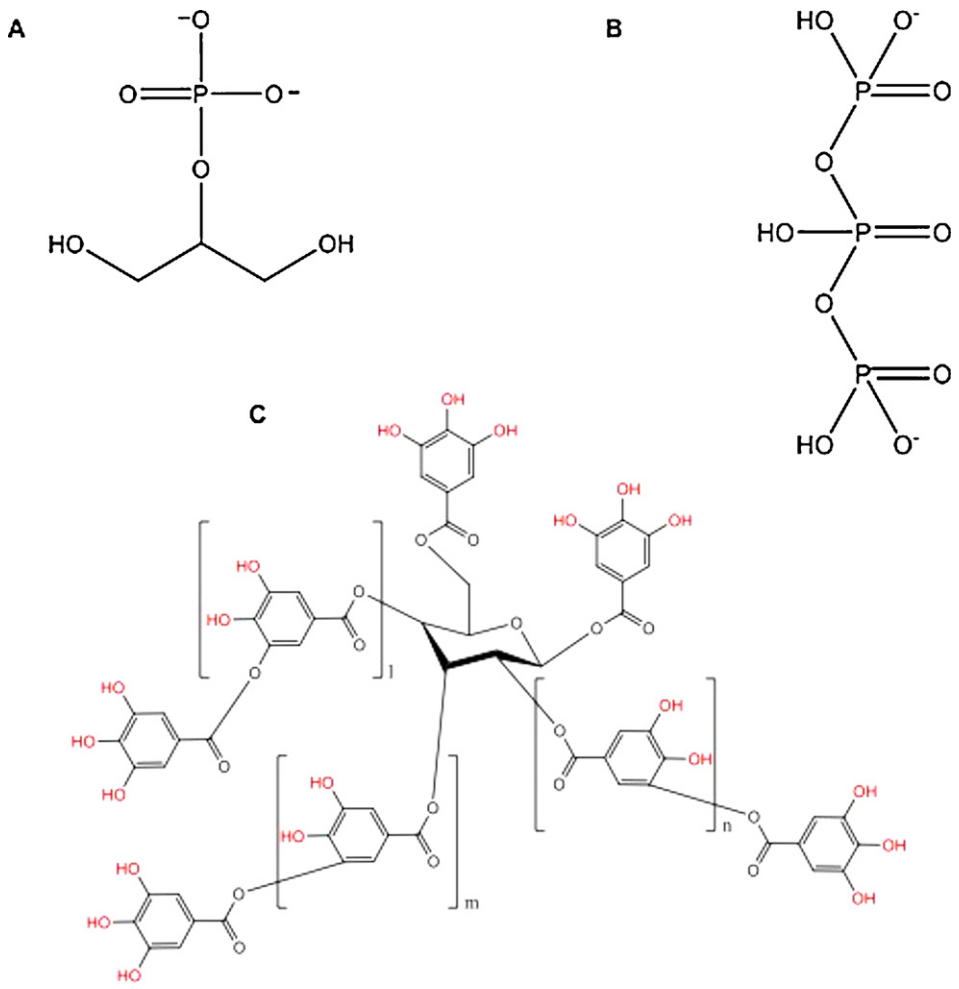

Fig. 1. Chemical structure of: (A) glycerol phosphate (GP); (B) tripolyphosphate (TPP); and (C) tannic acid (TA) ($l+m+n=0$–7).

2.3.4. Activated two-step

This method is a hybrid and modified version of both activated OS and TS crosslinking methods, in that after immersion of the as-spun chitosan mat into the crosslinker, the mats were exposed to heat- or base-activation. Activation and immersion procedures were the same as that of the activated OS and TS methods, respectively.

2.4. Viscosity, pH and conductivity of solutions

Viscosity of all the solutions used for electrospinning were measured based on the ASTM D446 standard method using an Ubbelohde glass capillary viscometer (Cannon Instrument Co., State College, PA).

Conductivity and pH of all the solutions were likewise measured prior to electrospinning. For the conductivity measurements however, the solutions were made with 1% TFA to prevent probe damage. An Oakton CON 5110 conductimeter (Vernon Hills, IL) and a universal range (pH 0-14) indicator sticks (J.T. Baker, Deventer, Netherlands) were utilized, respectively. All measurements were taken under ambient temperature ($25^\circ \pm 4^\circ$C) and three runs for each solution type.

2.5. Electrospinning of solutions

The chitosan or chitosan-crosslinker solution was loaded into a 10 mL syringe (Becton Dickinson & Co., Franklin Lakes, NJ, USA) and a 21-gauge Precision Glide needle (Becton Dickinson & Co., Franklin Lakes, NJ, USA) was attached. The syringe was placed on an advancement pump (Harvard Apparatus, Plymouth Meeting, PA) set at 0.5 mL/h flow rate and a distance of 10 cm from the collecting plate, which is a 90 mm × 90 mm copper plate wrapped with aluminum foil. A high voltage supply (Gamma High Voltage Research Inc., Ormond Beach, FL, USA) connects the needle (positive electrode) and the plate. A 15 kV applied voltage was used as the solution was advanced with the set flow rate. The setup was run at 23–25 °C and 30–35% RH. For comparison, chitosan solutions were spun (as-spun) as controls. All mats were carefully peeled off from the foil collector before any immersion or activation procedure was performed.

2.6. Field emission scanning electron microscopy (FESEM)

Fiber morphologies of the electrospun samples were observed under Zeiss Supra 50VP FESEM (Carl Zeiss NTS, LLC, North America) after coating the samples with platinum/palladium for 30 s and 40 mA using Denton Vacuum Desk II (Denton Vacuum, LLC, Moorestown, NJ, USA), depositing approximately a 5 nm thick coating. Mean fiber diameters ($N=50$) were measured using the ImageJ software (version 1.41o, National Institute of Health, USA). Fiber branching and web-like morphologies were also noted.

2.7. Fourier transform infrared microscopy (FTIR)

Infrared spectra of all fibers and bulks were recorded using FTIR (Varian Excalibur FTS-3000, Varian, Inc., Palo Alto, CA) with the

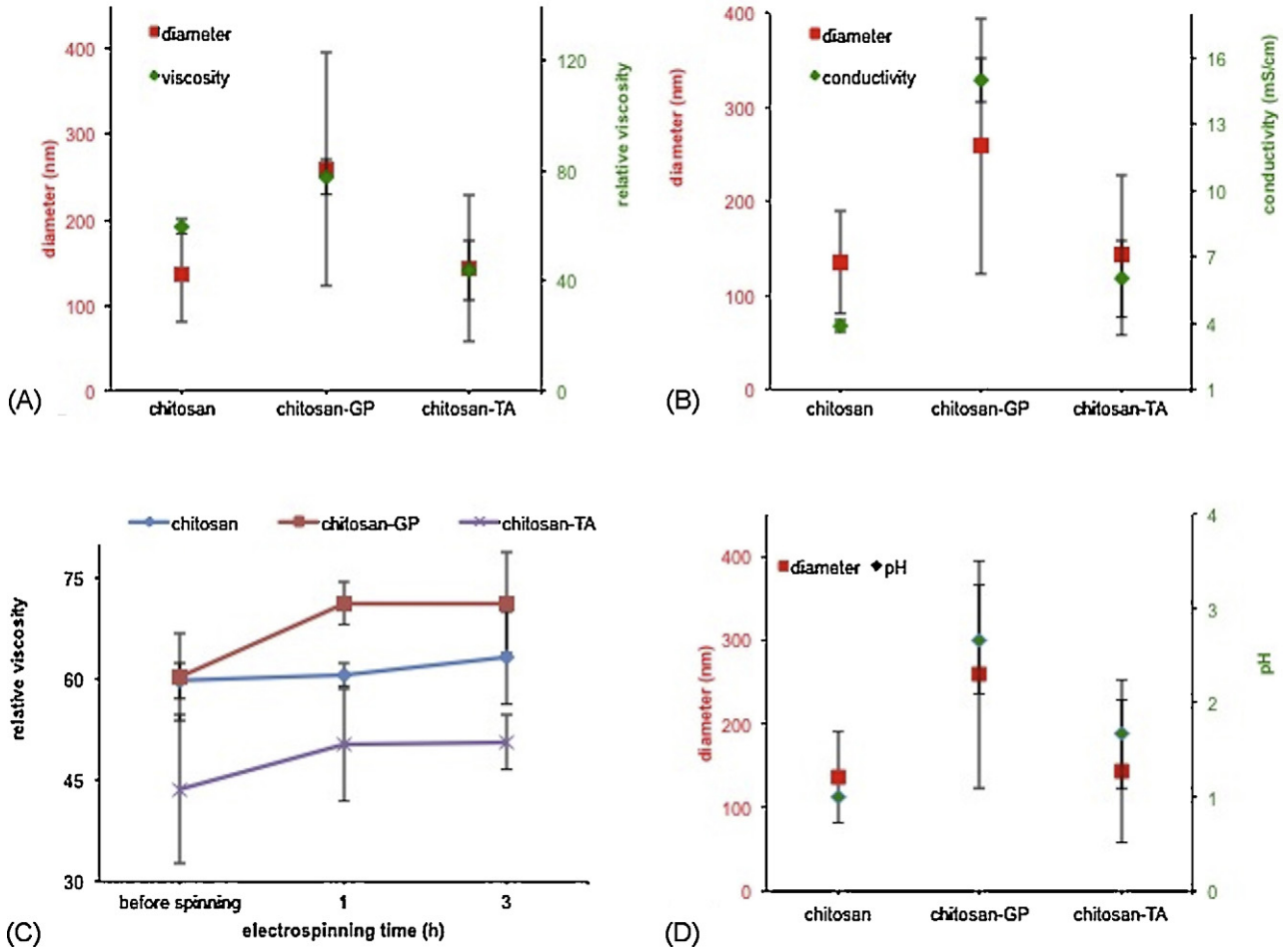

Fig. 2. Properties of chitosan-based solutions used for electrospinning: (A) relative viscosity; (B) relative viscosity at various electrospinning times; (C) conductivity; and (D) pH.

attenuated total reflectance (ATR) mode. All runs were done with a spectral range of 4000–500 cm^{-1} by accumulation of 64 scans at 4 cm^{-1} resolution.

2.8. Solubility test

Stability of the fiber mat samples was performed under acidic, neutral and basic solutions. Solubility test previously described by Austero et al. (2012) was modified and utilized to determine the stability of the fiber mats. Samples (0.5 mm × 0.5 mm) samples were cut from each mat and submerged in separate solutions each containing 20 mL solutions of 1 M AA (pH 3), distilled water (pH 7) and 1 M NaOH (pH 13) in square disposable Petri dishes (100 mm × 100 mm x 15 mm with 13 mm grid; Simport Plastics, QC, Canada). Mats were tested after 15 min and 72 h immersion under ambient conditions.

Mat dissolution was monitored by measuring the solution transmittance at 600 nm (T_{600}) using a spectrometer (USB2000 Miniature Fiber Optic Spectrometer, Ocean Optics, Inc., Dunedin, FL). All measurements were in triplicates. Values were normalized using 1 M AA, water and 1 M NaOH as reference solutions rather than the reference-crosslinker solutions (i.e. 1 M AA + GP). Moreover, all mats were visually observed (VO). Mats with $T_{600} \geq 90$ and VO = 100 indicate "not dissolved"; $T_{600} \geq 90$ and VO = 0 indicate "fully dissolved"; while those with $50 \leq T_{600} \leq 90$ and VO = 100 indicate "partially dissolved". Micrographs of the surface morphology of the mats that survived 72 h immersion in 1 M AA or water were taken using the FESEM.

2.9. Statistical analysis

All statistical analysis were performed on fiber diameters using StatPlus:Mac LE.2009 (Build 5.8.0.0, AnalystSoft Inc.) with p-level $\leq$0.05 as significant.

3. Results and discussion

All prepared chitosan, chitosan-GP and chitosan-TA solutions were electrospinnable. After 24 h mixing, chitosan-TFA solutions typically appear clear dark yellow to dark orange. The addition of GP (Fig. 1) to the chitosan-TFA solution did not contribute any color change while the addition of TA (Fig. 1) resulted to an opaque light yellow solution with grainy particles, most likely the TA molecules aggregating due to increased hydrophobic interactions at this low pH (Shutava et al., 2005). Fig. 2 displays the properties of the electrospinning solution. The increase in the relative viscosity of the chitosan-GP can be attributed to the chitosan chain conformation changing in the presence of the salt (Wyatt, Gunther, & Liberatore, 2011). Moreover, with the addition of GP (pK_a 6.26) and TA (pK_a 2.2–3.2), pH was observed to increase to 3 and 2, respectively. However, the spinning solution was not observed to gel even after 5 h of spinning. This is likely attributed to the crosslinkers remaining mostly uncharged at this low pH.

With TPP (Fig. 1) addition, the chitosan-TFA solution immediately (<1 min) formed a clear yellow gel that could not be electrospun. For this reason, TPP was only used for the TS

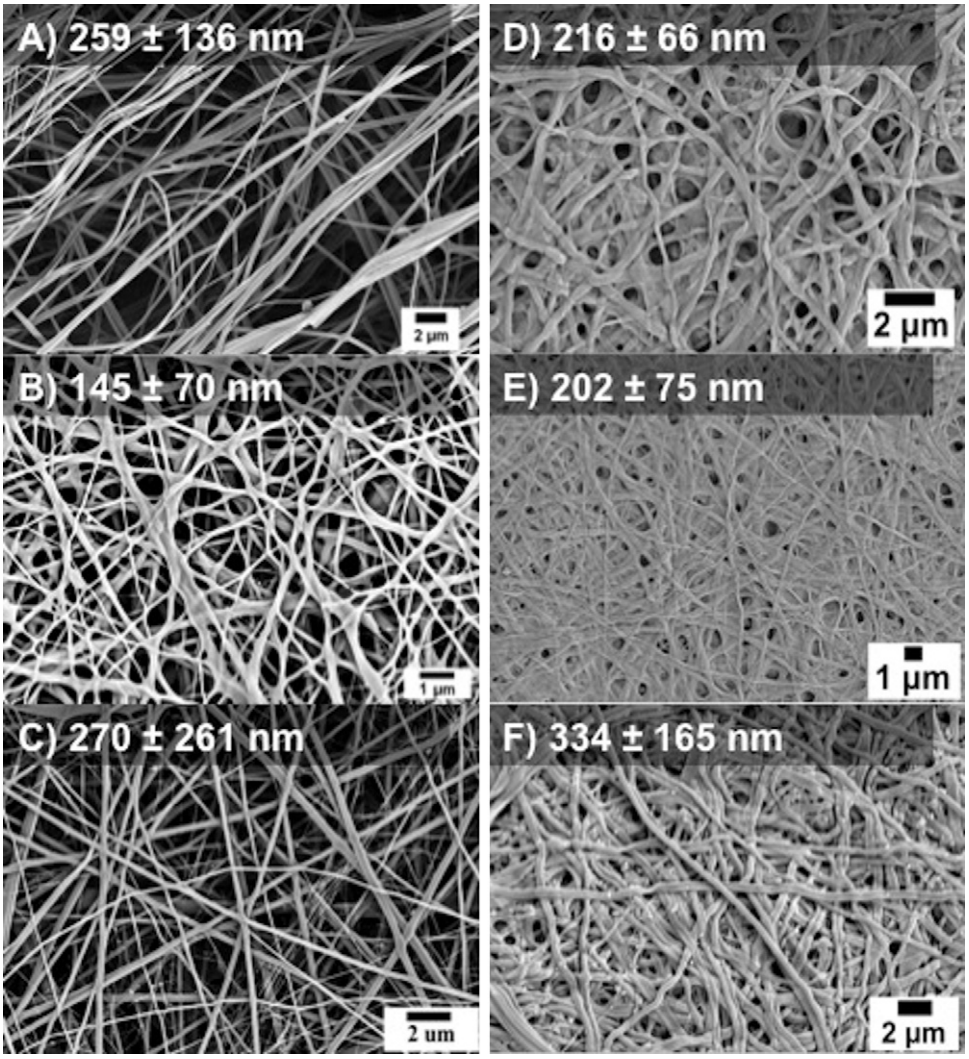

Fig. 3. FESEM micrographs of electrospun chitosan fiber mats: (A) chitosan-GP; (B) chitosan-GP-60 °C; (C) chitosan-GP-base; (D) TS chitosan-GP; (E) TS chitosan-GP-60 °C; and (F) TS chitosan-GP-base.

crosslinking of the chitosan fiber mats. The extensive and immediate crosslinking is likely due to the high charge density of TPP, having up to five negative charges per molecule as compared to GP with only one negative charge (Shu & Zhu, 2002a). Adjusting the TPP:chitosan ratio (i.e. reducing the concentration of TPP) or using blends of crosslinkers (Shu & Zhu, 2002a) have been proposed to either delay full crosslinking or keep the chitosan-TPP solution partially crosslinked to prevent immediate gelation and keep the solution electrospinnable.

3.1. Crosslinking chitosan fiber with GP

FESEM micrographs (Fig. 3) revealed smooth and ribbon-like OS chitosan-GP fibers with a mean fiber diameter of 259 ± 136 nm. This is a 95% increase in diameter from the as-spun chitosan (133 ± 53 nm) (Fig. 5). The increase in fiber diameter after OS crosslinking correlates with the data reported by Schiffman and Schauer (2007b) for the OS chitosan-GA. This increase in diameter can be attributed to the increased attractive forces between chitosan and GP, limiting jet elongation due to charge repulsion during fiber formation. Interestingly, even though an ionic crosslinker (i.e. one that can impart charges that can affect fiber formation during electrospinning) was added to our chitosan-TFA solution instead of the neutral, covalent crosslinker GA, the electrospinning parameters we used to fabricate the OS chitosan-GP was similar to what Schiffman and Schauer (2007b) had utilized.

Activation of the OS mats was performed to achieve chemical crosslinking of GP or TA with chitosan. High pH and increased temperature activation of previously studied chitosan crosslinkers have been observed to affect chitosan fiber diameters (Austero et al., 2012).

Due to the thermosensitivity of OS chitosan-GP mat, activation was performed by increased heat (60 °C, 24 h) (Cheng et al., 2010; Ruel-Gariepy et al., 2000, 2004; Ruel-Gariepy, Leclair, Hildgen, Gupta, & Leroux, 2002; Ruel-Gariepy & Leroux, 2006). After activation, the mean fiber diameter of the TS chitosan-GP-60 °C (145 ± 70 nm) (Fig. 3) decreased by 44% as a result of the possible removal of moisture on the mat plus the formation of more crosslinks. It is also important to note that the fibers have become highly branched and more web-like, indicating a possible increase in chain-to-chain interactions due to increased crosslinks between chitosan and GP (Filion, Lavertu, & Buschmann, 2007; Lavertu, Filion, & Buschmann, 2008). Increased fiber–fiber contact points due to covalent-crosslinking and activation of electrospun chitosan fibers have been reported to improve mechanical properties (Donius et al., 2013). Preliminary mechanical testing of the OS chitosan-GP (unbranched, individual) and TS chitosan-GP-60 °C (web) mats revealed higher tensile properties for the more

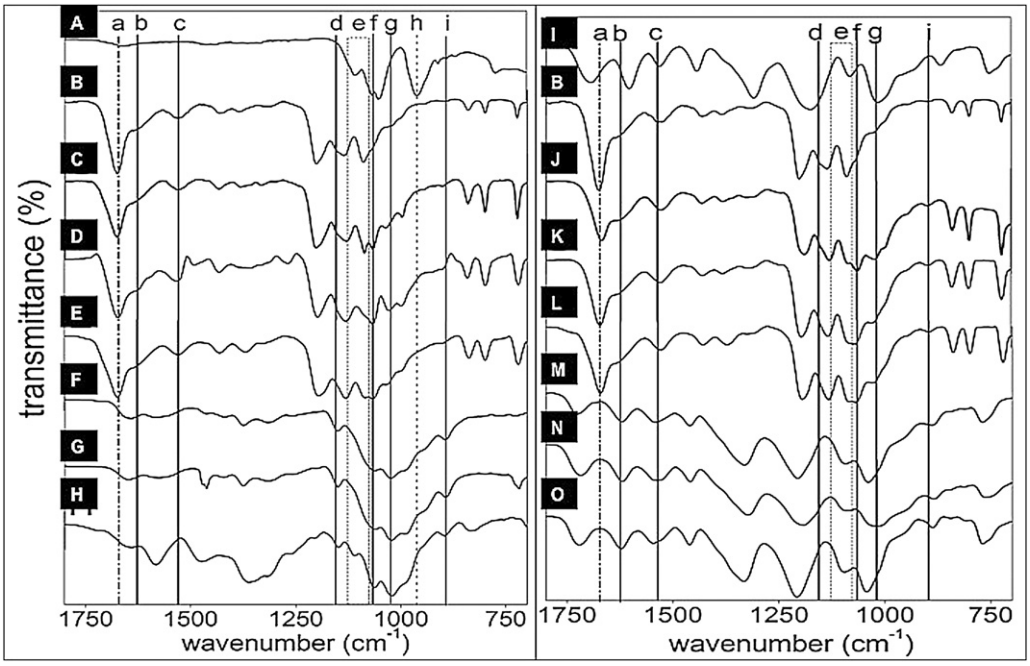

Fig. 4. FTIR spectra of bulk crosslinker or electrospun chitosan fiber mats: Left: (A) bulk GP; (B) chitosan; (C) chitosan-GP; (D) chitosan-GP-60 °C; (E) chitosan-GP-base; (F) TS chitosan-GP; (G) TS chitosan-GP-60 °C; (H) TS chitosan-GP-base; (I) bulk TA; (J) chitosan-TA; (K) chitosan-TA-60 °C, L) chitosan-TA-base; (M) TS chitosan-TA; (N) TS chitosan-TA-60 °C; and (O) TS chitosan-TA-base. Dashed vertical line (a) 1670 cm^{-1}, corresponds to the C=O of the residual TFA. Black solid vertical lines or box (e) are characteristic peaks of chitosan: (b) 1650 cm^{-1}, (c) 1560 cm^{-1}, (d) 1155 cm^{-1}, (f) 1060 cm^{-1}, (g) 1028 cm^{-1}; and (i) 890 cm^{-1}. Characteristic GP peak is at (h) 950 cm^{-1}.

branched mat. Tensile moduli were determined to be 52 MPa and 79 MPa while tensile strengths were 39 MPa and 66 MPa for OS chitosan-GP and TS chitosan-GP-60 °C, respectively.

Chitosan can crosslink with GP via the heat-induced transfer of protons from the protonated amine group of chitosan to the phosphate group of GP (Filion et al., 2007; Lavertu et al., 2008). By increasing the chitosan solution temperature from 5 to 85 °C, the apparent ionization constant (pK_{ap}) of chitosan decreases significantly by 0.023 pK_a units/°C, allowing the protonated amine groups to release its protons (Filion et al., 2007; Lavertu et al., 2008). Since the pK_a of GP is temperature-independent and close to that of the pK_{ap} of chitosan, it acts as a proton acceptor (Filion et al., 2007; Lavertu et al., 2008) forming these crosslinks. The formation of deprotonated amine groups is also proposed to reduce chain repulsion facilitating the precipitation or gelation of chitosan.

Interestingly, the base activation of TS chitosan-GP-base (Fig. 3) did not change the fiber morphology and only resulted to a minimal 4% increase in fiber diameter as compared to OS chitosan-GP, most likely due to uptake of moisture. In addition, even at a low concentration, the basic condition might have neutralized the still protonated amine groups of chitosan resulting to changes in the chain-to-chain repulsion (Lavertu et al., 2008).

To remove residual TFA that is present on the as-spun chitosan fiber, a neutralization step was performed. Neutralized as-spun chitosan mats are preferred not just for TS crosslinking but for post-processing techniques because this step ensures that more amine groups are available for subsequent reactions. Residual TFA ions on the mats are also undesirable for biocompatibility and safety reasons. The washing step was done to simply remove residual base and salts that may have formed due to neutralization of the mats with NaOH/ethanol.

After immersion into the GP solution, the TS chitosan-GP mat retained its fibrous structure with a mean fiber diameter of 216 ± 66 nm (Fig. 3) which is a 62% increase and 17% decrease when compared to as-spun chitosan and chitosan-GP mat, respectively. The increase in the diameter of as-spun chitosan mat after TS crosslinking was expected and in agreement to previous studies (Schiffman & Schauer, 2007a). The fiber diameter increase for the TS chitosan-GP from as-spun chitosan is not as large as the

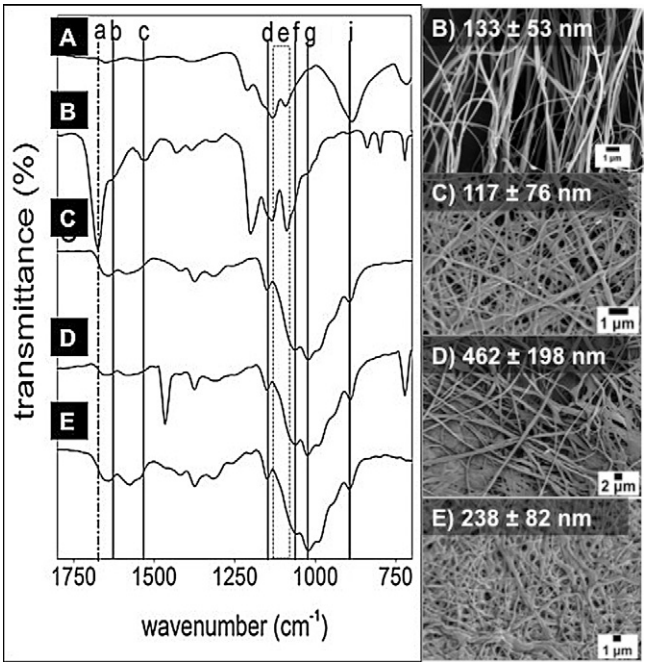

Fig. 5. FTIR spectra and FESEM micrographs of bulk TPP or electrospun chitosan fiber mats: (A) bulk TPP; (B) chitosan; (C) TS chitosan-TPP; (D) TS chitosan-TPP-60 °C; and (E) TS chitosan-TPP-base. Black vertical line (a) 1670 cm^{-1}, corresponds to the C=O of the residual TFA. Black solid vertical lines and box (e) correspond to the characteristic peaks of chitosan: (b) 1650 cm^{-1}, (c) 1560 cm^{-1}, (d) 1155 cm^{-1}, (f) 1060 cm^{-1}, (g) 1028 cm^{-1}, and (i) 890 cm^{-1}.

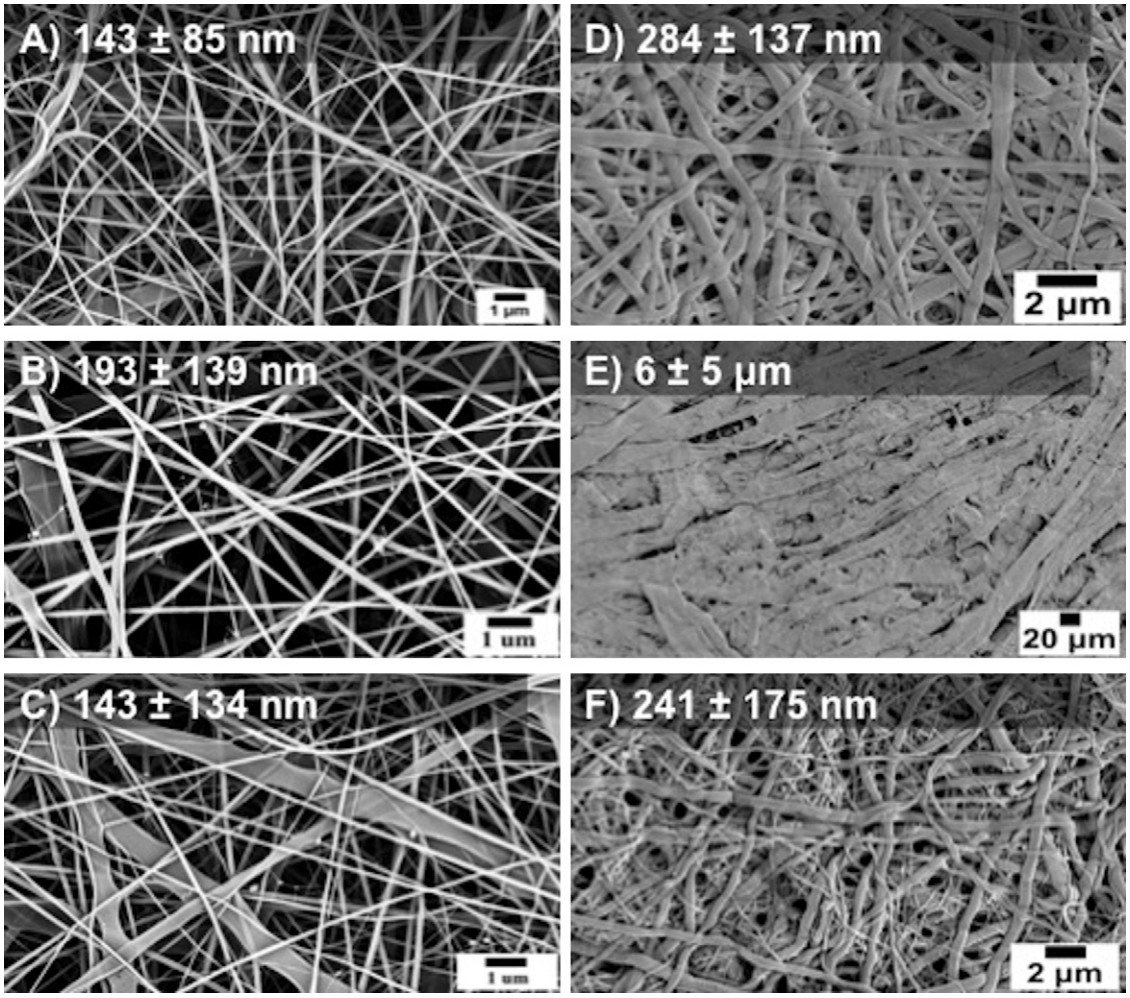

Fig. 6. FESEM micrographs of electrospun chitosan fiber mats: (A) chitosan-TA; (B) chitosan-TA-60 °C; (C) chitosan-TA-base; (D) TS chitosan-TA; (E) TS chitosan-TA-60 °C; and (F) TS chitosan-TA-base.

95% increase for the OS chitosan-GP. We suggest that due to the increased free amine and protonation of GP from sodium salt to OH groups now in the neutralized as-spun mat chain (i.e. amines during OS chitosan-GP are still protonated), the attractive interactions with the negatively charged GP in solution might have been reduced while the chain-to-chain hydrophobic attraction increased (Filion et al., 2007; Lavertu et al., 2008), resulting to smaller fiber diameters.

In Schiffman and Schauer's (2007a) previous work, activation after the TS crosslinking was not employed since GA readily crosslinks chitosan at acidic and ambient conditions. In our case, it was logical to perform an activation step after the TS method to provide optimum crosslinking conditions for GP or TA, apart from being able to compare the different post-processing and crosslinking methods. Like in OS chitosan-GP, activation of the TS chitosan-GP-60 °C mats resulted to a decrease in fiber diameters and may be attributed to the possible removal of moisture on the mat with the formation of more crosslinks. Branching and formation of more web-like fiber morphology was also noted, indicating a possible slight increase in chain-to-chain interactions due to increased crosslinks between chitosan and GP (Filion et al., 2007; Lavertu et al., 2008). On the other hand, the TS chitosan-GP-base had increased diameters but this may be due to absorbed moisture and not crosslinks, as will be explained later on in this paper under the FTIR and solubility test results.

3.1.1. FTIR of electrospun chitosan-GP fiber mats

To confirm the chemical crosslinking of GP, TPP or TA with chitosan, FTIR was performed (Figs. 4 and 5). As controls, FTIR spectra of the bulk reagents (chitosan, GP, TPP and TA) and as-spun mats were also taken. Both bulk and as-spun chitosan have the characteristic FTIR peaks: 3500–3200 cm^{-1} (NH, OH), 2850 cm^{-1} (CH), 1650 cm^{-1} (C=O of amide I), 1560 cm^{-1} (1° NH of amide II), 1450–1370 cm^{-1} (CH), 1155 cm^{-1} (COC), 1060 and 1028 cm^{-1} (CO) and 890 cm^{-1} (1° NH wag). Due to the broad OH stretch, the 1° amine peaks (3400–3500 cm^{-1}) were not distinct however the NH wag of the bulk chitosan indicates that amines are present.

The bulk GP spectrum displays characteristic peaks as well: 1050–1100 cm^{-1} (P=O) and 950 cm^{-1} (OH) (Boskey, Camacho, Mendelsohn, Doty, & Binderman, 1992). All the OS (chitosan-GP) and activated OS (chitosan-GP-60 °C and chitosan-GP-base) spectra of show characteristic chitosan and GP peaks however since the mats were not neutralized, the 1° amines are likely still protonated and did not show as NH_2 peaks in the spectra. This is confirmed by the strong peak at 1670 cm^{-1} and 1201 cm^{-1} (not highlighted), also present in the as-spun chitosan, which corresponds to the C=O and C—O respectively, of residual TFA and the loss of the NH_2 stretch and wag peaks for the electrospun mats. It should be noted that for the chitosan-GP-60 °C, although the NH_2 stretch peaks are not as pronounced due to the presence of the residual TFA, a slight increase in the NH_2 wag peak was observed with a shift and loss of

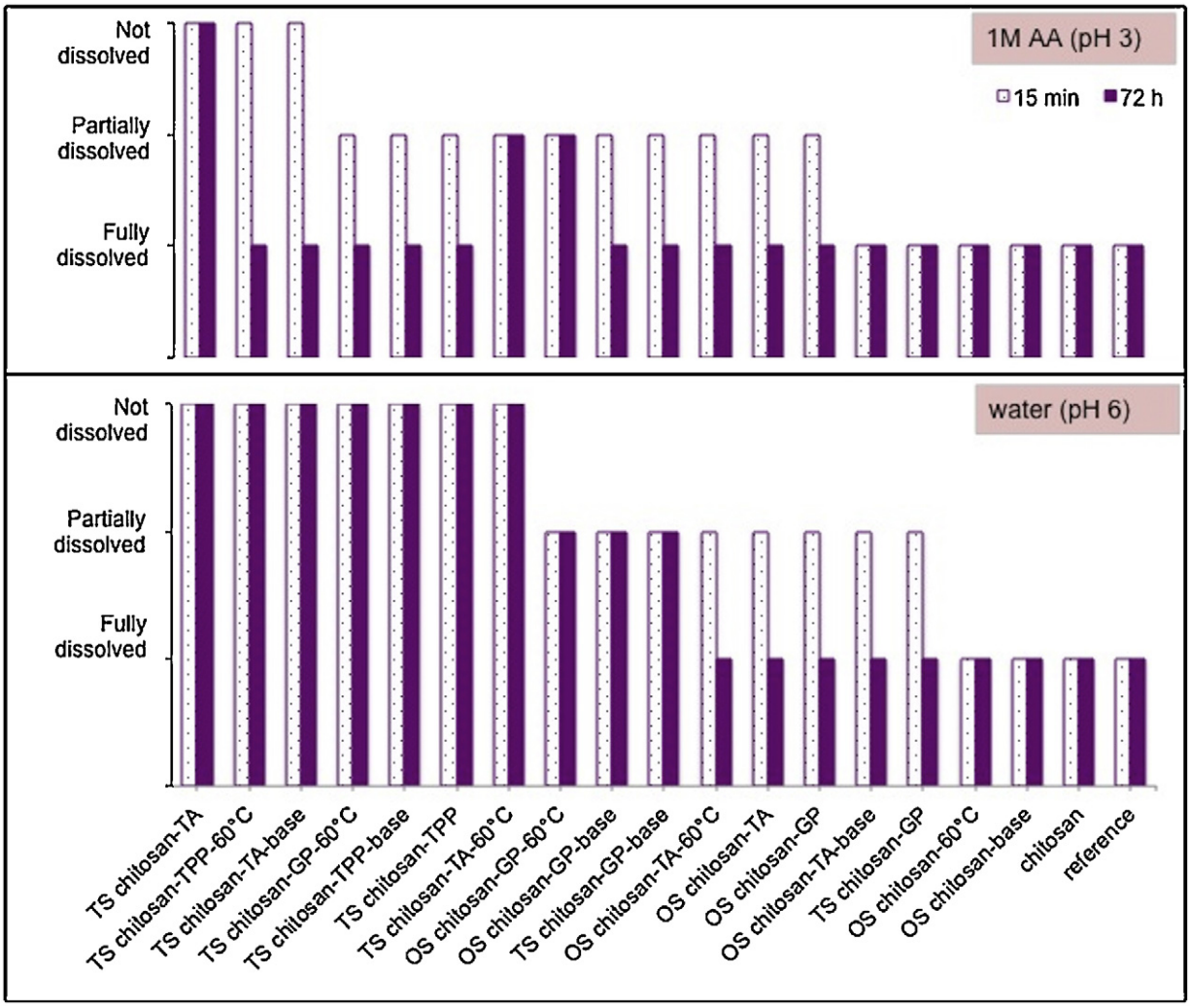

Fig. 7. Electrospun chitosan-based mat solubility in 1 M AA and water after 15 min and 72 h immersion.

the phosphate peaks, indicating the heat-induced transfer of protons from the protonated amines to GP (Filion et al., 2007; Lavertu et al., 2008).

To remove the residual TFA and prepare the as-spun mats for TS and activated TS crosslinking, the neutralization step was performed. Spectra of the neutralized as-spun and all the TS and activated TS mats displayed a loss of the TFA peaks and an increase in the NH_2 wag peak, indicating the deprotonation of the amine groups.

3.2. Crosslinking chitosan fiber with TPP

FESEM micrographs of all chitosan-TPP mats are displayed in Fig. 5. For TPP, only the TS and activated TS methods were employed since TPP crosslinks at a shorter period of time than GP after mixing with chitosan-TFA. Moreover, unlike GP, chitosan-TPP interaction is not heat activated. For this paper, we added heat activation and base activation after TS chitosan-TPP to determine if these conditions enhance crosslinking. This immediate crosslinking, attributed to the strong phosphate groups of TPP forming ionic bonds with the amine groups of chitosan, poses a challenge when trying to electrospin in OS as it clogs the syringe and needle when the solution fully gels and turns yellow.

In contrast to the fiber diameter trend of the TS chitosan-GP mats, the TS chitosan-TPP mats have an opposite trend, with the TS chitosan-TPP-60 °C having the largest diameter at 462 ± 198 nm (247% larger than as-spun chitosan) (Fig. 5), most likely due to faster chitosan-TPP interaction at higher temperatures. Unlike TS chitosan-GP, the TS chitosan-TPP yielded smaller fibers (12% smaller than as-spun chitosan) after immersing into the TPP solution. As for the base-exposed mat, the fiber diameter slightly increased compared to as-spun chitosan (by 79%) and TS chitosan-TPP (by 103%). We suggest that apart from the crosslinking, the moisture and presence of base influenced the diameter increase and poor chemical stability in acidic medium (Fig. 7). Chitosan-TPP-based materials (i.e. beads) are known to be pH responsive (i.e. swells at various pHs), however the sensitivity of these depends on the concentration of TPP and chitosan, crosslinking time (Shu & Zhu, 2002a, 2002b, 2002c) and the degree of deacetylation of chitosan.

3.2.1. FTIR of electrospun chitosan-TPP fibers

The FTIR spectra of TS chitosan-TPP fiber mats are shown in Fig. 5. Characteristic TPP peaks were observed for the bulk TPP. The loss of the residual TFA peak of the spun mats was also noticeable in the spectra. In acidic conditions (~pH 3), the phosphoric groups of TPP are highly involved in the crosslinking with the amine group of chitosan. This was indicated in the spectra as an increase in the height, broadening and shifting to lower wavenumbers (1100–1200 cm^{-1}) for the phosphate groups.

(A)

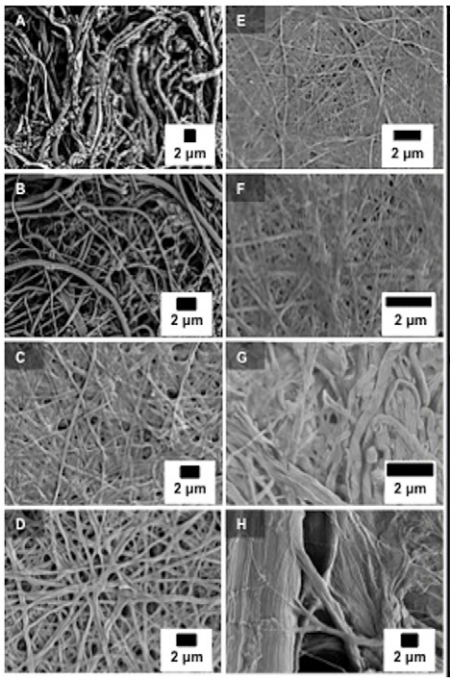

(B)

water solubility	composition	fiber diameter (nm)	initial mat morphology
not dissolved	TS chitosan-TA	284 ± 137	individual/web
	TS chitosan-TPP-60°C	462 ± 198	web
	TS chitosan-TA-base	241 ± 175	web
	TS chitosan-GP-60°C	202 ± 75	branched/web
	TS chitosan-TPP-base	238 ± 82	web
	TS chitosan-TPP	117 ± 76	web
	TS chitosan-TA-60°C	5554 ± 4975	web
partially dissolved	OS chitosan-GP-60°C	145 ± 70	web
	OS chitosan-GP-base	270 ± 261	individual
	TS chitosan-GP-base	334 ± 165	branched/web
	OS chitosan-TA-60°C	193 ± 139	individual
	OS chitosan-TA	143 ± 85	individual
	OS chitosan-GP	259 ± 136	individual
	OS chitosan-TA-base	143 ± 134	individual
	TS chitosan-GP	216 ± 66	branched/web

Fig. 8. (a) FESEM micrographs of electrospun mats after 72 h solubility test.1 M AA (A) and water (B–H): (A) TS chitosan-TA; (B) TS chitosan-TA; (C) TS chitosan-TPP-60 °C; (D) TS chitosan-TA-base; (E) TS chitosan-GP-60 °C; (F) TS chitosan-TPP-base; (G) TS chitosan-TPP; and (H) TS chitosan-TA-60 °C. (b) Summary of the various electrospun and crosslinked mat compositions with corresponding water solubility after 72 h, fiber diameters and fiber mat morphology.

3.3. Crosslinking chitosan fiber with TA

FESEM micrographs of all chitosan-TA mats are displayed in Fig. 6. Like the OS GP-containing mats, the fiber diameters of the OS TA mats have the same trend. Chitosan-TA mat yielded a non-uniform, smooth and ribbon-like to round fibers having smaller mean fiber diameters of 143 ± 85 nm, only an 8% increase in diameter from the as-spun chitosan mat control (133 ± 53 nm) (Fig. 5). In comparison to the mean fiber diameter of as-spun chitosan, the chitosan-TA-60 °C was 45% higher. As will be explained later in this paper under the FTIR section for TA and supported by chemical stability data, these changes in chitosan fiber diameters may not be due to chemical crosslinking interactions with TA but by the effects of moisture in the fibers.

As expected, diameter of the TS chitosan-TA mat was 114% larger than as-spun chitosan. Interestingly, the web-like TS chitosan-TA-60 °C fiber mat had even larger fiber diameters at 6 ± 5 μm while the TS chitosan-TA-base fibers are smaller at 241 ± 174 nm (81% higher than as-spun chitosan) (Fig. 6). This trend is opposite to what was observed with the TS GP-containing mats but in agreement to the TS chitosan-TPP mats.

3.3.1. FTIR of electrospun chitosan-TA fibers

FTIR spectra (Fig. 4) of the TA bulk powder, as-spun chitosan mat and TA-containing mats were taken. The presence of numerous hydroxyl, benzene rings and carbonyl functional groups on the TA structure lead to the numerous peaks in the spectra. These peaks are characteristic of TA. Crosslinking chitosan with TA most likely does not involve covalent bonding but is instead a result of multiple weak hydrogen bonds. Previous studies have reportedly used TA to crosslink chitosan microparticles (Aelenei, Popa, Novac, Lisa, & Balaita, 2009). It is also important to note that naturally, bulk chitosan contains tannins that are not fully removed during the processing of chitosan from chitin material of crustaceans. This may result to possible difficulty in trying to deconvolute the individual contributions of chitosan or TA functional groups in the spectrum.

The presence of residual TFA on the OS chitosan-TA mats was also observed. Also, other than the changes around the C—O—C peaks for the chitosan-TA, chitosan-TA-60 °C and chitosan-TA-base, the spectra did not indicate any possible crosslinking interaction. The broadening and shift to a lower wavenumber for these peaks indicate possible H-bonding. The changes in fiber diameters associated with the addition of TA and activation conditions are possibly due to water loss by heating (i.e. decrease in diameter) or neutralization of the tannic acid (i.e. increase in diameter) for the chitosan-TA-60 °C and chitosan-TA-base, respectively.

Unlike the OS TA mats, the spectra of the TS and activated TS TA mats showed some changes in the peak locations and heights. In addition to characteristic chitosan and TA peaks, the shift to lower wavenumber and increase in peak height of the 1650 cm^{-1} peak of chitosan is assigned to the symmetrical deformations of NH_3^+ as a result of protonation of the primary amine group in the presence of COO^- of TA. The acidity of the solution and the presence of protonated amine groups may have resulted to the hydrolysis of TA leading to the formation of carboxylic group-containing gallic dimers (Aelenei et al., 2009). The broad single band at around 1330 cm^{-1} was observed for all three TS mats. The COC bonding vibrations also broadened and shifted to lower wavenumber. The 1647 cm^{-1} band of TA was displaced to 1727 cm^{-1} and a formation of a weak 1461 cm^{-1} peak, assigned to the COO^-) were observed. These changes in the spectra indicate the strong ionic interactions between the carboxyl groups of TA and the amine groups of chitosan (Aelenei et al., 2009), leading to the very large increase in fiber diameters and improved chemical stability as compared to the OS mats.

3.4. Solubility of electrospun fiber mats

Fig. 7 shows the solubility of all electrospun mats in 1 M AA (pH 3), water (pH 6) and 1 M NaOH (pH 13) while Fig. 8A displays the

representative FESEM images of the fibers post 72 h solubility test in either 1 M AA or water. FTIR and the stability data correlated and confirmed the full and partial crosslinking of the various mats. Knowing that chitosan is insoluble only at high pH due to amine groups being deprotonated, mat insolubility at neutral to acidic conditions would indicate partial to full crosslinking. Solubility tests indicated that after 72 h at pH 3, TS chitosan-TA did not dissolve, suggesting full crosslinking. At close to neutral pH, TS chitosan-TPP-60 °C, TS chitosan-TA-base, TS chitosan-GP-60 °C, TS chitosan-TPP-base, TS chitosan-TPP and TS chitosan-TA-60 °C mats survived 72 h.

3.5. Mat composition, fiber structure and solubility property

Fig. 8B summarizes the various electrospun and crosslinked mat compositions, solubility in water and fiber mat morphology. The OS or TS approach to crosslinking of electrospun chitosan fibers with GP, TPP and TA influenced the fiber surface morphologies and the chemical interactions or solubility in aqueous solutions of pH 3–6. The OS or activated OS process created mostly unbranched, individual fibers that partially dissolve in pH 3–6, indicating only partial crosslinking due to the presence of residual trifluoroacetate ions from the solvent. In contrast, the TS or activated TS approach created more branched to web-like fibrous mats with most not dissolving in water.

This wide range of stabilities in addition to the various fiber morphology and diameters produced by varying the crosslinking technique, mat compositions and crosslinker type is promising for various applications such as filtration, tissue engineering and drug delivery systems.

4. Conclusion

Taken as a whole, chitosan crosslinked with GP, TPP or TA using four various methods exhibits a wide range of fiber morphology and fiber diameter characteristics. Chitosan-GP-60 °C, TS chitosan-TA and TS chitosan-TA-60 °C demonstrated stable and uniformly fibrous mat. As for TPP and TA, the TS method was observed to produce smaller and more chemically stable fibers than the OS method.

This paper enhances the number of potential electrospun chitosan crosslinkers from purely covalent to ionic versions leading to designed properties depending on the required application. To date, these are the first reported electrospinning of GP-, TPP- or TA-crosslinked chitosan fiber mats. Future studies are geared toward determining the mechanical stability of the fiber mats and exploring their use as filter membranes or tissue engineering scaffolds.

Acknowledgements

The authors thank: Dr. Edward Basgall and the Centralized Research Facilities (CRF), College of Engineering, Drexel University for use of FESEM and the sputter coater; Dr. Giuseppe Palmese for the use of the ATR-FTIR; MAK thank the Institute of Food Technologists (PA section) and Drexel University Freshmen Design Engineering Fellowship 2010–2013; The authors wish to acknowledge funding by the NSF CMMI grant no. 0804543 and Ben Franklin Nanotechnology Institute, Philadelphia, PA.

References

Aelenei, N., Popa, M. I., Novac, O., Lisa, G., & Balaita, L. (2009). Tannic acid incorporation in chitosan-based microparticles and in vitro controlled release. *Journal of Materials Science-Materials in Medicine*, *20*(5), 1095–1102.

An, J. H., & Dultz, S. (2007). Adsorption of tannic acid on chitosan-montmorillonite as a function of pH and surface charge properties. *Applied Clay Science*, *36*(4), 256–264.

Austero, M. S., Donius, A. E., Wegst, U. G. K., & Schauer, C. L. (2012). New crosslinkers for electrospun chitosan fibre mats. I. Chemical analysis. *Journal of the Royal Society Interface*, *9*(75), 2551–2562.

Barry, J. E., Finkelstein, M., & Ross, S. D. (1984). Hydrogen-bonded complexes. 5. Phenol amine complexes. *Journal of Organic Chemistry*, *49*(9), 1669–1671.

Berger, J., Reist, M., Mayer, J. M., Felt, O., Peppas, N. A., & Gurny, R. (2004). Structure and interactions in covalently and ionically crosslinked chitosan hydrogels for biomedical applications. *European Journal of Pharmaceutics and Biopharmaceutics*, *57*(1), 19–34.

Boskey, A. L., Camacho, N. P., Mendelsohn, R., Doty, S. B., & Binderman, I. (1992). FT-IR microscopic mappings of early mineralization in chick limb bud mesenchymal cell-cultures. *Calcified Tissue International*, *51*(6), 443–448.

Brack, H. P., Tirmizi, S. A., & Risen, W. M. (1997). A spectroscopic and viscometric study of the metal ion-induced gelation of the biopolymer chitosan. *Polymer*, *38*(10), 2351–2362.

Chang, M. Y., & Juang, R. S. (2004). Adsorption of tannic acid, humic acid, and dyes from water using the composite of chitosan and activated clay. *Journal of Colloid and Interface Science*, *278*(1), 18–25.

Charlton, A. J., Baxter, N. J., Khan, M. L., Moir, A. J. G., Haslam, E., Davies, A. P., et al. (2002). Polyphenol/peptide binding and precipitation. *Journal of Agricultural and Food Chemistry*, *50*(6), 1593–1601.

Cheng, Y. H., Yang, S. H., Su, W. Y., Chen, Y. C., Yang, K. C., Cheng, W. T. K., et al. (2010). Thermosensitive chitosan-gelatin-glycerol phosphate hydrogels as a cell carrier for nucleus pulposus regeneration: An in vitro study. *Tissue Engineering Part A*, *16*(2), 695–703.

Chenite, A., Buschmann, M., Wang, D., Chaput, C., & Kandani, N. (2001). Rheological characterisation of thermogelling chitosan/glycerol-phosphate solutions. *Carbohydrate Polymers*, *46*(1), 39–47.

Devi, N., & Maji, T. K. (2009). Effect of crosslinking agent on neem (Azadirachta Indica A. Juss.) seed oil (NSO) encapsulated microcapsules kappa-carrageenan and chitosan polyelectrolyte complex. *Journal of Macromolecular Science Part a-Pure and Applied Chemistry*, *46*(11), 1114–1121.

Donius, A. E., Kiechel, M. A., Schauer, C. L., & Wegst, U. G. K. (2013). New crosslinkers for electrospun chitosan fibre mats. Part II: Mechanical properties. *Journal of the Royal Society Interface*, *10*(81).

Du, W. L., Niu, S. S., Xu, Y. L., Xu, Z. R., & Fan, C. L. (2009). Antibacterial activity of chitosan tripolyphosphate nanoparticles loaded with various metal ions. *Carbohydrate Polymers*, *75*, 385–389.

Faikrua, A., Jeenapongsa, R., Sila-asna, M., & Viyoch, J. (2009). Properties of beta-glycerol phosphate/collagen/chitosan blend scaffolds for application in skin tissue engineering. *ScienceAsia*, *35*(3), 247–254.

Filion, D., Lavertu, M., & Buschmann, M. D. (2007). Ionization and solubility of chitosan solutions related to thermosensitive chitosan/glycerol-phosphate systems. *Biomacromolecules*, *8*(10), 3224–3234.

Fukada, H., & Takahashi, K. (1998). Enthalpy and heat capacity changes for the proton dissociation of various buffer components in 0.1 M potassium chloride. *Proteins: Structure Function and Genetics*, *33*(2), 159–166.

Kumar, M., Muzzarelli, R. A. A., Muzzarelli, C., Sashiwa, H., & Domb, A. J. (2004). Chitosan chemistry and pharmaceutical perspectives. *Chemical Reviews*, *104*(12), 6017–6084.

Lavertu, M., Filion, D., & Buschmann, M. D. (2008). Heat-induced transfer of protons from chitosan to glycerol phosphate produces chitosan precipitation and gelation. *Biomacromolecules*, *9*(2), 640–650.

Lopez-Leon, T., Carvalho, E. L. S., Seijo, B., Ortega-Vinuesa, J. L., & Bastos-Gonzalez, D. (2005). Physicochemical characterization of chitosan nanoparticles: Electrokinetic and stability behavior. *Journal of Colloid and Interface Science*, *283*(2), 344–351.

Madhan, B., Dhathathreyan, A., Subramanian, V., & Ramasami, T. (2003). Investigations on geometrical features in induced ordering of collagen by small molecules. *Proceedings of the Indian Academy of Sciences-Chemical Sciences*, *115*(5–6), 751–766.

Muzzarelli, R. A. A. (2009). Genipin-crosslinked chitosan hydrogels as biomedical and pharmaceutical aids. *Carbohydrate Polymers*, *77*(1), 1–9.

Muzzarelli, R. A. A., Boudrant, J., Meyer, D., Manno, N., DeMarchis, M., & Paoletti, M. G. (2012). Current views on fungal chitin/chitosan, human chitinases, food preservation, glucans, pectins and inulin: A tribute to Henri Braconnot, precursor of the carbohydrate polymers science, on the chitin bicentennial. *Carbohydrate Polymers*, *87*(2), 995–1012.

Muzzarelli, R. A. A., Greco, F., Busilacchi, A., Sollazzo, V., & Gigante, A. (2012). Chitosan, hyaluronan and chondroitin sulfate in tissue engineering for cartilage regeneration: A review. *Carbohydrate Polymers*, *89*(3), 723–739.

Osawa, R., & Walsh, T. P. (1993). Effects of acidic and alkaline treatments on tannic-acid and its binding property to protein. *Journal of Agricultural and Food Chemistry*, *41*(5), 704–707.

Reneker, D. H., Yarin, A. L., Zussman, E., & Xu, H. (2007). Electrospinning of nanofibers from polymer solutions and melts. In H. Aref, & E. VanDerGiessen (Eds.), *Advances in applied mechanics* (pp. 43–195). Oxford: Elsevier.

Ruel-Gariepy, E., Chenite, A., Chaput, C., Guirguis, S., & Leroux, J. C. (2000). Characterization of thermosensitive chitosan gels for the sustained delivery of drugs. *International Journal of Pharmaceutics*, *203*(1–2), 89–98.

Ruel-Gariepy, E., Leclair, G., Hildgen, P., Gupta, A., & Leroux, J. C. (2002). Thermosensitive chitosan-based hydrogel containing liposomes for the delivery of hydrophilic molecules. *Journal of Controlled Release*, *82*(2-3), 373–383.

Ruel-Gariepy, E., & Leroux, J. C. (2006). Chitosan: A natural polycation with multiple applications. In R. H. Marchessault, F. Ravenelle, & X. X. Zhu (Eds.), *Polysaccharides for drug delivery and pharmaceutical applications* (pp. 243–259). Portland: Book News, Inc.

Ruel-Gariepy, E., Shive, M., Bichara, A., Berrada, M., Le Garrec, D., Chenite, A., et al. (2004). A thermosensitive chitosan-based hydrogel for the local delivery of paclitaxel. *European Journal of Pharmaceutics and Biopharmaceutics*, *57*(1), 53–63.

Schiffman, J. D., & Schauer, C. L. (2007a). Cross-linking chitosan nanofibers. *Biomacromolecules*, *8*(2), 594–601.

Schiffman, J. D., & Schauer, C. L. (2007b). One-step electrospinning of cross-linked chitosan fibers. *Biomacromolecules*, *8*(9), 2665–2667.

Schiffman, J. D., & Schauer, C. L. (2008). A review: Electrospinning of biopolymer nanofibers and their applications. *Polymer Reviews*, *48*(2), 317–352.

Shu, X., & Zhu, K. J. (2000). A novel approach to prepare tripolyphosphate/chitosan complex beads for controlled release drug delivery. *International Journal of Pharmaceutics*, *201*(1), 51–58.

Shu, X. Z., & Zhu, K. J. (2001). Chitosan/gelatin microspheres prepared by modified emulsification and ionotropic gelation. *Journal of Microencapsulation*, *18*(2), 237–245.

Shu, X. Z., & Zhu, K. J. (2002a). Controlled drug release properties of ionically-crosslinked chitosan beads: The influence of anion structure. *International Journal of Pharmaceutics*, *23*, 217–225.

Shu, X. Z., & Zhu, K. J. (2002b). The influence of multivalent phosphate structure on the properties of ionically-crosslinked chitosan films for controlled drug release. *European Journal of Pharmaceutics and Biopharmaceutics*, *54*, 235–243.

Shu, X. Z., & Zhu, K. J. (2002c). The release behavior of brilliant blie from calcium-alginate gel beads coated by chitosan: The preparation method effect. *European Journal of Pharmaceutics and Biopharmaceutics*, *53*, 193–201.

Shu, X. Z., Zhu, K. J., & Song, W. H. (2001). Novel pH-sensitive citrate cross-linked chitosan film for drug controlled release. *International Journal of Pharmaceutics*, *212*(1), 19–28.

Shutava, T., Prouty, M., Kommireddy, D., & Lvov, Y. (2005). pH responsive decomposable layer-by-layer nanofilms and capsules on the basis of tannic acid. *Macromolecules*, *38*(7), 2850–2858.

Shutava, T. G., & Lvov, Y. M. (2006). Nano-engineered microcapsules of tannic acid and chitosan for protein encapsulation. *Journal of Nanoscience and Nanotechnology*, *6*(6), 1655–1661.

Van Buren, J. P., & Robinson, W. B. (1969). Formation of complexes between protein and tannic acid. *Journal of Agricultural and Food Chemistry*, *17*(4), 772–777.

Wyatt, N. B., Gunther, C. M., & Liberatore, M. W. (2011). Increasing viscosity in entangled polyelectrolyte solutions by the addition of salt. *Polymer*, *52*(11), 2437–2444.